Journal of Cellular Physiology

Rab7 Regulates CDH1 Endocytosis, Circular Dorsal Ruffles Genesis, and Thyroglobulin Internalization in a Thyroid Cell Line

ANNA MASCIA,[1] FLAVIANA GENTILE,[1] ANTONELLA IZZO,[2] NUNZIA MOLLO,[2] MARIA DE LUCA,[3] CECILIA BUCCI,[3] LUCIO NITSCH,[2] AND GAETANO CALÌ[1]*

[1]*IEOS Istituto di Endocrinologia e Oncologia Sperimentale "G. Salvatore", National Council of Research, Napoli, Italy*

[2]*Department of Molecular Medicine and Medical Biotechnologies, University "Federico II", Napoli, Italy*

[3]*Department of Biological and Environmental Sciences and Technologies, University of Salento (DiSTeBA), Lecce, Italy*

Rab7 regulates the biogenesis of late endosomes, lysosomes, and autophagosomes. It has been proposed that a functional and physical interaction exists between Rab7 and Rac1 GTPases in CDH1 endocytosis and ruffled border formation. In FRT cells over-expressing Rab7, increased expression and activity of Rac1 was observed, whereas a reduction of Rab7 expression by RNAi resulted in reduced Rac1 activity, as measured by PAK1 phosphorylation. We found that CDH1 endocytosis was extremely reduced only in Rab7 over-expressing cells but was unchanged in Rab7 silenced cells. In Rab7 under or over-expressing cells, Rab7 and LC3B-II co-localized and co-localization in large circular structures occurred only in Rab7 over-expressing cells. These large circular structures occurred in about 10% of the cell population; some of them (61%) showed co-localization of Rab7 with cortactin and f-actin and were identified as circular dorsal ruffles (CDRs), the others as mature autophagosomes. We propose that the over-expression of Rab7 is sufficient to induce CDRs. Furthermore, in FRT cells, we found that the expression of the insoluble/active form of Rab7, rather than Rab5, or Rab8, was inducible by cAMP and that cAMP-stimulated FRT cells showed increased PAK1 phosphorylation and were no longer able to endocytose CDH1. Finally, we demonstrated that Rab7 over-expressing cells are able to endocytose exogenous thyroglobulin via pinocytosis/CDRs more efficiently than control cells. We propose that the major thyroglobulin endocytosis described in thyroid autonomous adenomas due to Rab7 increased expression, occurs via CDRs.

J. Cell. Physiol. 9999: 1–14, 2015.

Families of Rab and Rho GTPases are known to regulate many cellular functions: intracellular trafficking, cell proliferation, cell-cell and cell-substrate adhesion (Lozano et al., 2003; Bryant and Stow, 2004; Jaffe and Hall, 2005; Stenmark, 2009). Rab7 is a small GTPase of the Rab family, first identified in a rat liver cell line (Bucci et al., 1988). Rab7 regulates late endocytic traffic from the biogenesis of lysosomes and phagolysosomes, to the maturation of late autophagic vacuoles (Bucci et al., 2000; Harrison et al., 2003; Jager et al., 2004). Rab7 is also important for cell nutrition and apoptosis (Edinger et al., 2003; Snider, 2003).

It has been shown that a molecular, functional (Frasa et al., 2010) and physical (Sun et al., 2005) interaction between Rab7 and Rac1 in CDH1 endocytosis and ruffled border formation exists. It has been proposed that the Tre/Bub2/Cdc16/rab GTPase-activating protein (TBC/RabGAP) Armus, integrates signaling between Arf6, Rac1, and Rab7 during junction disassembly. Armus specifically binds to activated Rac1 and its C-terminal TBC/RabGAP domain inactivates Rab7 and regulates CDH1 endocytosis (Frasa et al., 2010). The Rac1 activation state in CDH1 endocytosis is still debated. It has also been demonstrated that CDH1 endocytosis is regulated by the activity state of CDH1 through activation of the Rac/Cdc42-IQGAP1 system induced by CDH1 trans interaction (Izumi et al., 2004). Moreover it has been demonstrated that Rac1 activation leads to phosphorylation of its effector PAK1 (Manser et al., 1994; Knaus et al., 1995) and that Rac1 activity is also involved in actin cytoskeleton modification needed for the genesis of Circular Dorsal Ruffles (CDRs).

CDRs are membrane protrusions composed of actin-rich structures and are formed on the apical surfaces of cells. Putative functions of CDRs are the internalization of

Abbreviations: AJ, adherent junctions; Ap, apical; AU, arbitrary units; Bl, basolateral; BSA, bovine serum albumin; cAMP, cyclic adenosine monophosphate; CDH1, cadherin 1 E-cadherin; CDRs, circular dorsal ruffles; DQ5, DRAQ5; ECL, enhanced chemioluminescence; FRT, fischer rat thyroid; FSK, forskolin; HRP, horse radish peroxidase; IBMX, 3-Isobutyl-1-methylxanthine; kDa, kilodalton; IF, immunofluorescence; LC3B-II, microtubule-associated protein light chain 3-II; O/N, overnight; PAK1, P21 protein (Cdc42/Rac)-activated kinase 1; PMSF, phenylmethylsulfonyl fluoride; SD, standard deviation; SDS–PAGE, sodium dodecyl sulphate–polyacrylamide gel electrophoresis; TBC/RabGAP, Tre/Bub2/Cdc16/rab GTPase-activating protein; TCA, trichloroacetic acid; TER, trans epithelial resistance; Tg, thyroglobulin; WB, western blot.

Anna Mascia and Flaviana Gentile contributed equally to this work.

Conflicts of interest: The authors have nothing to disclose.

Contract grant sponsor: MIUR-PRIN 2012.
Contract grant sponsor: AIRC;
Contract grant number: IG2013 N.14709.

*Correspondence to: Gaetano Calì, Institute of Endocrinology and Molecular Oncology of CNR, Via S. Pansini 5, 80131 Naples, Italy.
E-mail: g.cali@ieos.cnr.it

Manuscript Received: 27 July 2015
Manuscript Accepted: 23 November 2015

Accepted manuscript online in Wiley Online Library (wileyonlinelibrary.com): 00 Month 2015.
DOI: 10.1002/jcp.25267

substrates, receptors and membrane, and cell motility. Their genesis is induced by growth factor stimulation but the molecular mechanism involved in CDRs formation has not been fully elucidated and it is not clear how the actin cytoskeleton is organized in the CDRs. Some actin-related proteins are reported to co-localize with the actin ring in CDRs such as cortactin, dynamin, N-WASP, and Arp2/3 (Krueger et al., 2003; Orth et al., 2006; Palamidessi et al., 2008). In epithelioid cells, the Rab5 GTPase is required, in addition to Rac1, for the genesis of CDRs: disruption of Rac1 and Rab5 signals impairs the formation of CDRs (Palamidessi et al., 2008).

In the thyroid, hormone production by thyrocytes following thyroglobulin endocytosis and intracellular processing in late endosomes/lysosomes suggests that its rate can be regulated by the expression or function of Rab5 and Rab7; a putative binding site for a cAMP response element has been found on the Rab5 and Rab7 gene promoters. In thyroid autonomous adenomas, where the cAMP cascade is constitutively activated, increased expression of Rab5 and Rab7 has been observed (Croizet-Berger et al., 2002). It is well known that the architecture of thyroid tissues is deeply modified by c-AMP stimulation with the production of pseudopods and the formation of intracellular colloid droplets in the apical compartment of cells (Pastan and Wollman, 1967).

In this paper, we investigate the role of the Rab7, Rac, PAK1, CDH1 axis in endocytosis in FRT cells. We show that Rab7 over-expression causes increased expression and activity of Rac1, whilst Rac1 activity is decreased in FRT cells in which Rab7 expression is reduced by RNAi, as measured by PAK1 phosphorylation. We find that CDH1 endocytosis is extremely reduced only in Rab7 over-expressing cells but is unchanged in Rab7-silenced cells. In Rab7 over-expressing cells, LC3B-II protein and Rab7 co-localize on large circular structures. We observe these large circular structures in about 10% of the cell population, some of them (61%) show co-localization of Rab7 with cortactin and f-actin and are identified as circular dorsal ruffles (CDRs), while the others are mature autophagosomes. We propose that the over-expression of Rab7 alone is sufficient to induce CDRs. The insoluble/active form of Rab7 is inducible by cAMP, and cAMP-stimulated FRT cells show increased PAK1 phosphorylation and are no longer able to endocytose CDH1. Rab7 over-expressing cells are able to endocytose exogenous thyroglobulin via CDRs and we propose that the major thyroglobulin endocytosis described in thyroid autonomous adenomas, in which cAMP signal is constitutively activated, may occur via CDRs.

Materials and Methods

Antibodies

The following antibodies were used: mouse monoclonal anti-CDH1 (1:1000 Western blotting (WB) and immunoprecipitation (IP) and mouse monoclonal anti-Rab8 (1:1000 WB) BD Transduction Laboratories, Franklin Lakes, NJ; mouse monoclonal anti-Rab7 (1:1000 WB) and mouse monoclonal anti-α-tubulin (1:5000 WB) Sigma–Aldrich, St. Louis, MO; mouse monoclonal anti-Rab7 (1:100 IF) and rabbit polyclonal anti-Rab5 (1:100 IF; 1:1000 WB) Santa Cruz Biotechnology, Dallas, TX; rabbit polyclonal antibodies anti-LC3B-II (1:400 IF; 1:1000 WB) was a gift from A. Puca (University of Salerno) and anti-Beclin-1 (1:1000 WB) Cell Signaling Technology, Denvers, MA; mouse monoclonal anti-Rac1 (1:1000 WB) Upstate, Lake Placid, NY; rabbit polyclonal anti-PAK p-T^{423} (1:1000 WB) Invitrogen, Carlsbad, CA; rabbit polyclonal anti cortactin (1:100 IF) was a gift from A. De Matteis (TIGEM, Naples); rabbit polyclonal anti-thyroglobulin (1:100 IF; 1:5000 WB) was a gift from R. Di Lauro (University Federico II, Naples); Alexa Fluor 488 and 546 goat anti-rabbit and anti-mouse (1:200 IF) (Molecular Probes, Leiden, The Netherlands); and horseradish peroxidase-conjugated goat anti rabbit and goat anti mouse (1: 2000 WB) Amersham, Little Chalfont, Buckinghamshire, UK.

Cell culture

FRT cells (Mascia et al., 1997) were cultured in plastic culture dishes or on polyester filters in bicameral systems (Costar, Corning, Inc., The Netherlands) in Coon's modified Ham's F-12 medium (Euroclone) supplemented with 5% fetal calf serum (HyClone, Thermo Scientific, Erembodegem, Belgium). FRTL5 cells were grown in the same medium supplemented with 5% calf serum and a mixture of six hormones and growth factors (6 H) as previously described (Mascia et al., 1997). Cultures were kept at 37°C in a humidified atmosphere of 5% CO_2 and 95% air.

Generation of stable cell lines

FRT cells were transfected with pCDNA3.1 mcherry Rab7 or sh-RNA Rab7 plasmids. The pCDNA3.1 mcherry Rab7 plasmid was previously published (Progida et al., 2006), while sh-RNA Rab7 plasmid was from Origene Technologies (TI743701, cat. No. TR710925). Stable cell lines transfected with the mCherry-Rab7 plasmid or with sh-RNA Rab7 plasmid were selected with G-418 (1 mg/ml, Calbiochem) or puromycin (3 mg/ml, Sigma–Aldrich), respectively. Cells were kept in selective media for about two weeks or until clones were visible. Clones were then picked, propagated and lysed. Extracts were processed for Western blotting in order to verify Rab7 overexpression or silencing. After selection, clones over-expressing mcherry-Rab7 were cultured in medium supplemented with 0.25 mg/ml G418 while Rab7-silenced clones were maintained in medium supplemented with 0.75 μg/ml puromycin.

Immunofluorescence and confocal microscopy

Cultured cells grown on coverslips were fixed in 4% paraformaldehyde in PBS for 20 min, washed twice in 50 mM NH_4Cl in PBS, and permeabilized for 5 min in 0.2% Triton X-100 in PBS. Alternatively, for the Rab5/Rab7 colocalization experiments, cells were fixed in TCA 10% at 4°C for 15 min, washed in Glycine 30 mM in PBS and permeabilized for 5 min in 0.2% Triton X-100 in PBS; for LC3B-II staining, cells were fixed in methanol at −20°C for 10 min and in acetone at −20°C for 1 min. Fixed and permeabilized cells were treated as described (Cali et al., 2012). Nuclei were stained with the DNA intercalator DRAQ5 (Alexis Corp., Lausen, Switzerland). IF analysis was performed with a confocal laser scanning microscope LSM 510 Meta (Zeiss, Gottingen, Germany). The λ of the argon ion laser was set at 488 nm, and that of the two HeNe lasers was set at 543 and at 633 nm. Fluorescence emission was revealed by 505–530 band pass filter for Alexa Fluor 488, by 560–615 band pass filter for Alexa Fluor 546, and by 615 long pass filter for DRAQ5. Double and triple staining IF images were acquired separately in the green, red, and infrared channels at a resolution of 1024 × 1024 pixels, with the confocal pinhole set to one Airy unit and then saved in TIFF format. Experiments were performed at least in triplicate.

Western blotting

Western blots were performed as described (Cali et al., 2007). Protein levels were quantified by densitometry using ImageJ software (http://imagej.nih.gov/ij/) and normalized against α-tubulin. Experiments were performed at least in triplicate.

Endocytosis assay

Sh1, FRT, and mCH5 confluent cell monolayers growth on filter chambers (Costar) were washed 5× with PBS/CM (PBS containing 0.1 mM Ca 2+ and 1 mM Mg 2+) at 4°C. A cleavable biotin

analogue, sulfosuccinimyl 2-(biotinamido) ethyl-l, 3 dithioproprionate (NHS-SS-biotin; Pierce Chemical Co. Thermo Scientific, Rockford, IL) (0.5 mg/ml in PBS/CM; freshly diluted from a frozen stock of 200 mg/ml in DMSO) was added to the basolateral compartment of the filter chamber. Labeling was for 20 min at 4°C and repeated twice. After the final labeling, filter chambers were washed twice with F12 Coon's mod/0.2% BSA. Two filters were kept on ice, the others transferred to 37°C for various times (20, 40, 60, 120 min). Incubation was stopped by transferring filters back to 4°C. After two washes in PBS/10% serum filters were incubated twice for 20 min in reducing solution: 310 mg glutathione (free acid) dissolved in 17 ml H_20; 1 ml of 1.5 M NaCl, 0.12 ml of 50% NaOH and 2 ml of serum added just before use (Bretscher and Lutter, 1988). One filter was mock treated. After washing, free SH-groups were quenched in 5 mg/ml iodoacetamide in PBS/1% BSA for 15 min. Filters were excised from the chamber with a scalpel and extracted with 1 ml of RIPA buffer (1% Igepal, 0.5% deoxycholate, 0.1% SDS, 150 mM NaCl, 50 mM Tris-HCl, pH 7.4 containing protease inhibitors (cOmplete mini, Roche, Mannheim, D) and 2 mM PMSF.

The cell lysate was pre-cleared with 1 ml 10 mg/ml swelled protein-A-sepharose (CL 4B) (GE Healthcare, Buckinghamshire, UK) for 1 h at 4°C and incubated with 1 μl of anti CDH1 antibody for 16 h at 4°C. Soluble immunocomplexes were bound to protein-A-sepharose and recovered by centrifugation. The samples were eluted by boiling the pellets in SDS–PAGE sample buffer without 2-mercapto ethanol. 10% SDS–PAGE was performed under non-reducing conditions. After SDS–PAGE, proteins were transferred to nitrocellulose (Protran, Amersham GE healthcare, Buckinghamshire, UK) in a Bio-Rad apparatus (Bio-Rad). Blots were blocked for 1 h with 5 % BSA in TTBS (20 mM Tris HCl pH 7.4; 150 mM NaCl, 0.1% Tween 20) at room temperature. HRP-Streptavidin (Amersham GE Healthcare, Buckinghamshire, UK) (1:1000 in TTBS) was allowed to bind for 1 h at room temperature, followed by washing in TTBS (4× for 15 min each). Blots were dried and developed using ECL detection method (Pierce Chemical Co. Thermo Scientific, Rockford, IL) according to the manufacturer's instructions.

RNA extraction and quantitative real-time PCR

Total RNA from each sample was extracted using TRIzol reagent (Gibco/BRL Life Technologies, Inc., Gaithersburg, MD) and was reverse transcribed using the iScript cDNA Synthesis kit (Bio-Rad Laboratories, Inc., Hercules, CA). Real-time PCR was performed using SsoAdvanced universal SYBR Green supermix on CFX96 Touch Real-Time PCR Detection System according to the manufacturer's protocols. PCR reactions were performed in triplicate. Primer pairs (MWG Biotech, Ebersberg, Germany) were designed using the Primer 3 software (http://frodo.wi.mit.edu/primer3) to obtain amplicons ranging from 100 to 150 base pairs. Expression values were normalized to unstimulated FRT cells. The G6PDH housekeeping gene was chosen as reference gene. Primer sequences: RAB7A-Forward: AGGTCATCATCCTGGGAGACT, RAB7A-Reverse: TGGCTTTGTACTGGTTACTGAACTT, G6PD-Forward: TTA TCA TCA TGG GTG CAT CG, G6PD-Reverse: AAG GTG TCT CTT CGG GTA GAA GG.

Statistical analysis

Student's *t*-test was applied to evaluate the statistical significance of differences measured throughout the data presented. The threshold for statistical significance (*P*-value) was set at 0.05.

Results

Rab7 expression

Thyroid epithelial polarized and undifferentiated rat thyroid cells FRT (Cali et al., 1998) were stably transfected either with cDNA coding for Rab7 fused with mCherry fluorescent protein or with a plasmid containing short hairpin (sh)-RNA specific to rat Rab7 to down-regulate its expression. Several stable clones were obtained and cell lysates were screened by Western blot (WB) for Rab7 expression with a mouse monoclonal antibody recognizing both endogenous and transfected Rab7 protein. WB results and the normalized densitometric quantitation are shown in Figure 1A and B, respectively. We selected the Sh Rab7 clone 1, showing approximately 40% downregulation in Rab7 expression compared to wild type FRT cells, and Rab7 mCherry clone 5, showing 60% upregulation of the protein (hereafter identified as Sh1 and mCH5, respectively) for further analysis. Results of immunofluorescence and confocal microscopy analysis with mouse monoclonal antibody anti Rab7 in FRT, Sh1 and mCH5 cells were in good agreement with WB results. Rab7 antibody staining was less intense in Sh1 and stronger in mCH5 compared to FRT cells (Fig. 1C: A, D, and H), complete co-localization of anti Rab7 antibody staining and autofluorescence of Rab7 mCherry was also observed (Fig. 1C: G and H). DQ5 nuclear staining (Fig. 1C: B, E, and I) and Merge (Fig. 1C: C, F, and J) are also shown.

Rab7 and Rac1 activation

It is well known that the small GTPase Rac is responsible for actin cytoskeleton remodeling and cell migration (Machesky and Hall, 1997; Kjoller and Hall, 2001). It has been proposed that Rac plays a pivotal role in intracellular traffic and that its intracellular localization is important for determining the site(s) at which its signaling occurs (Del Pozo and Schwartz, 2007).

FRT, Sh1, and mCH5 cell lysates were analyzed by SDS PAGE and WB for Rac1 protein expression. To obtain indirect evidence of Rac1 activity, we analyzed the phosphorylation state of p21 activated protein (PAK), a serine/threonine protein kinase activated by Cdc42 and Rac1 (Manser et al., 1994) that is a down-stream Rac activated effector (del Pozo et al., 2000; Bokoch, 2003; Stockton et al., 2004). In mCH5 cells, Rac1 expression was upregulated, whereas Sh1 cells expressed similar levels of Rac compared to parental FRT cells. In FRT and in Sh1 cells, Rac1 protein was almost inactive and unable to phosphorylate the threonine 423 of PAK, whereas mCH5 cells showed increased phosphorylation state of PAK^{T423}, in agreement with the greater Rac1 expression. As a loading control, WB analysis with anti α-tubulin antibodies is also shown (Fig. 2A). Normalized densitometric quantitation of WB signals are shown in Figure 2B.

Rab7 expression modulates CDH1 endocytosis

In a polarized epithelium, the integrity of adherens junctions (AJ) is crucial to prevent epithelial cell migration. CDH1 is the main structural protein of the AJ. Rac1 plays a major role in CDH1 endocytosis and in the remodeling of adhesive contacts (Palacios et al., 2001; Paterson et al., 2003). CDH1 endocytosis is a Rac-regulated process: it has been debated whether it is enhanced (Akhtar and Hotchin, 2001; Frasa et al., 2010) or inhibited (Izumi et al., 2004) by Rac activation. Since a molecular and functional link between Rab7 and Rac1 exists, we questioned whether there were differences in CDH1 endocytosis in FRT, Sh1, and mCH5 cells. We performed a classical endocytosis assay as described by Graeve et al. (1989). Cells grown on filters in bicameral system were biotinylated with a cleavable form of biotin (S-S Biotin), as described in the Materials and Methods. Remarkably, endocytosis of CDH1 occurred with similar kinetics in FRT and in Sh1 cells, while it was almost totally abolished in mCH5, as shown by the detection of immunoprecipitated CDH1, revealed by HRP conjugated streptavidin (Fig. 3A). As a loading control, the same

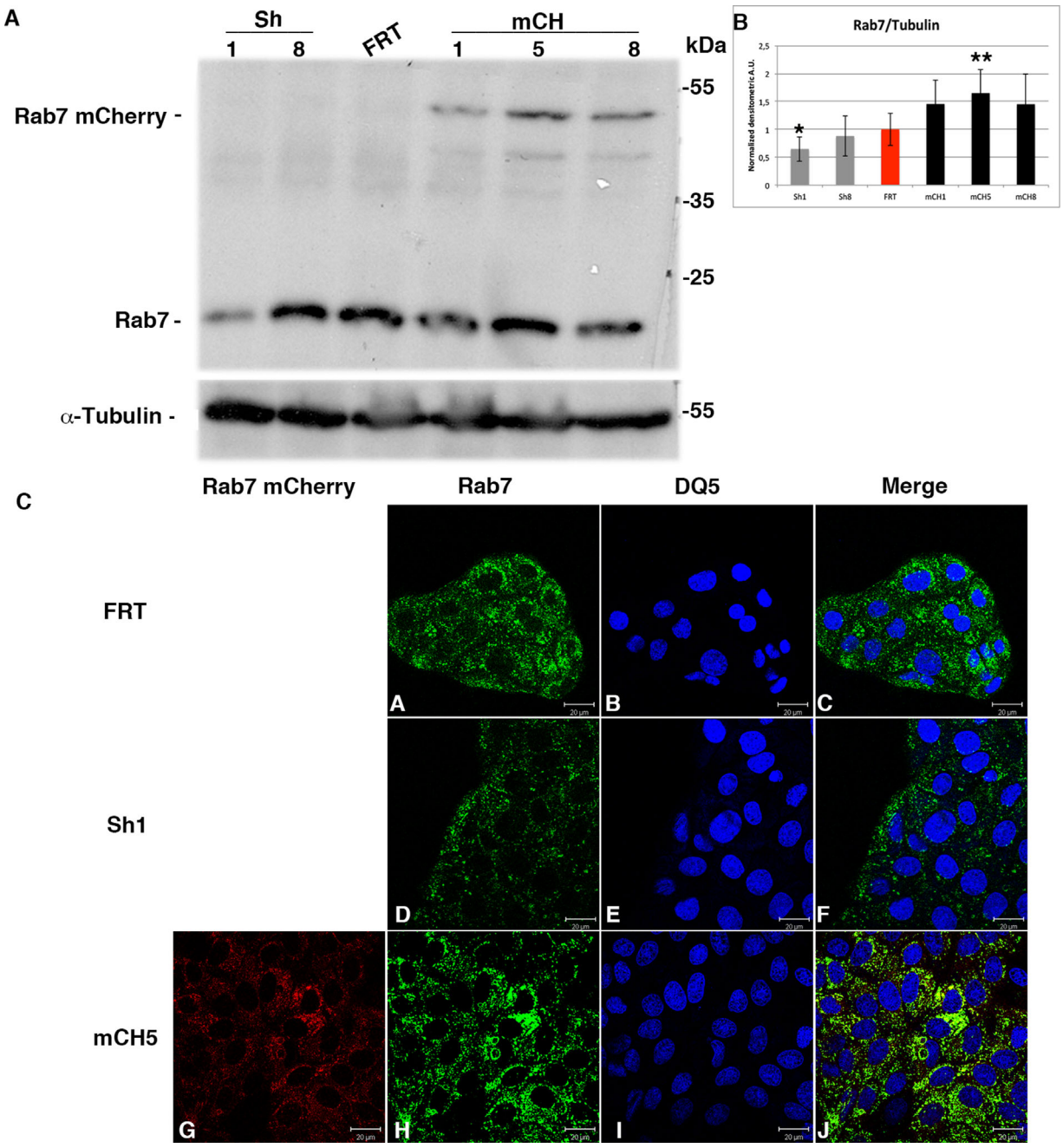

Fig. 1. Rab7 expression in FRT cells and in transfected clones. A: WB of cell lysates of Sh, FRT, and mCH cells with mouse monoclonal antibodies anti-Rab7 and after stripping, as loading control, with monoclonal anti-α-tubulin antibodies. Rab7 expression was efficiently down-regulated only in the Sh1 clone while good over-expression occurred only in mCH5 clone. B: α-tubulin normalized densitometric measurements (±SD) of resolved bands showed that in Sh1 cells, Rab7 expression was down-regulated by about 40%, whilst in mCH5 cells, Rab7 expression was up-regulated by more than 60% compared to FRT untransfected cells. $^{*}P = 0.05$ for Sh1 versus FRT comparison; $^{**}P < 0.05$ for mCH5 versus FRT comparison. *P*-values express statistical significance. C: Immunofluorescence staining of FRT (A–C), Sh1 (D–F), and mCH5 (G–J) cells with mouse monoclonal antibodies anti Rab7 (A, D, H), autofluorescent Rab7 m-Cherry staining of mCH5 cells (G), DQ5 nuclear staining (B, E, I) and Merge (C, F, J) are shown. Rab7 antibodies stained a vesicular compartment in the analyzed cell line. Rab7 staining was less intense in Sh1 cells (D) and more intense in mCH5 cell (H) compared to FRT cells (A). In mCH5 cells, co-localization between the transfected Rab7-mCherry and endogenous Rab7 was complete. Images are representative of at least five different experiments.

filter was stripped and hybridized with an anti-CDH1 antibody showing that steady state plasma membrane CDH1 is very similar across the examined clones (Fig. 3B). Densitometric analysis of the rate of CDH1 endocytosis is also shown (Fig. 3C).

Rab7 over-expression induces autophagic vacuoles genesis

A role for Rab7 in the final maturation of late autophagic vacuoles was proposed (Jager et al., 2004). LC3B-II is a soluble

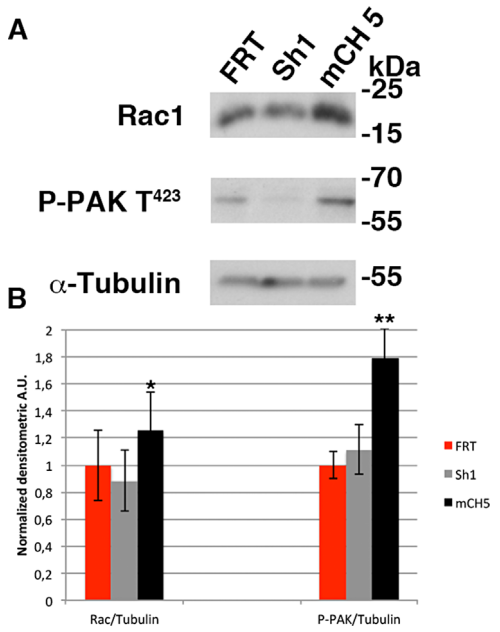

Fig. 2. Rac1 protein is over-expressed and hyper-active in mCH5 cells. A: WB of cell lysates of Sh, FRT, and mCH5 cells with mouse monoclonal antibodies anti-Rac1 and after stripping with rabbit polyclonal antibodies anti-PAK p-T^{423} and as loading control, with monoclonal antibodies anti α-tubulin. B: α-tubulin normalized densitometric measurements (±SD) of resolved bands showed that Rac1 expression was up-regulated in mCH5 cells. Also expression of phosphorylated kinase PAK, a downstream Rac activated effector, was up-regulated. $^{*}P = 0.05$ $^{**}P < 0.01$. P-values express statistical significance for mCH5 versus FRT comparisons.

protein that is ubiquitously distributed in mammalian tissues and cultured cells, which is recruited to autophagosomal membranes. It is considered a marker for autophagy (Tanida et al., 2008). We stained FRT and Sh1 cells with antibodies against LC3B-II (Fig. 4A and E) and Rab7 (Fig. 4B and F), while only antibodies to LC3B-II (Fig. 4I) were used on the mCH5 Rab7-Cherry autofluorescent cells (Fig. 4J). Nuclei were stained with DQ5 (Fig. 4C, G, and K). In FRT cells, LC3B-II and Rab7 co-localized in part on small vesicles and on rare circular structures (Fig. 4A–D). In Sh1 cells, LC3B-II, and Rab7 proteins also co-localized; small vesicles were visible and large circular structures were not seen (Fig. 4E–H). In the mCH5 clone over-expressing Rab7, staining for LC3B-II and Rab7 showed numerous large circular structures in addition to co-localization of the two markers, although only some of these structures were both LC3B-II and Rab7 mCherry positive (Fig. 4I, J, and L). These results indicated that over-expression of the Rab7 protein was able to induce an increase of large mature autophagosomes and also the generation of large circular structures.

We investigated the expression of proteins known to be regulated in autophagocytosis in FRT, Sh1, and mCH5 cell lysates by SDS PAGE and WB with antibodies anti LC3B-II, Beclin-1 and Rab5. mCH5 cells up regulated the expression of proteins playing a central role in autophagy. WB confirmed, according to the immunofluorescence results, that the expression of LC3B-II was up-regulated. Other than LC3B-II, mCH5 cells up-regulated the expression of Beclin 1, a protein that intervenes at every major step in autophagic pathways: from autophagosome formation, to autophagosome/endosome maturation (Kang et al., 2011; Wang et al., 2012).

We did not find any substantial differences between mCh5 and Sh1 cells in the expression level of Rab5, a protein involved in the early endocytotic pathway that regulates membrane traffic into and between early endosomes. Its downstream regulation has a very high level of complexity and might regulate other aspects of endosome function in addition to docking and fusion (Christoforidis et al., 1999). Densitometric normalized quantitation of WB results is also shown (Supplementary Fig. S1A and B).

Rab7 over-expression induces circular dorsal ruffles genesis

Circular dorsal ruffles, podosomes and invadopodia are the sites where actin remodeling occurs. We tested the hypothesis that Rab7 would be required for the generation of circular dorsal ruffles (CDRs) in thyroid epithelial cells. It has been described that cortactin has a predominant role in circular dorsal ruffle formation (Buccione et al., 2004). To this end, we looked by triple immunofluorescence and confocal microscopy for the localization/organization of f-Actin, cortactin and Rab7 in FRT, Sh1 and in mCh5 cells, specifically addressing what occurs on the dorsal (apical) side of the cells. In FRT cells, falloidin stained the cortical ring of Actin and only some of the large circular structures (Fig. 5A), such structures were more evident if stained by the anti Rab7 (Fig. 5B) and anti-cortactin antibodies (Fig. 5C). In Sh1 cells, falloidin stained the cortical ring of Actin and small circular structures (Fig. 5E), while the anti-Rab7 antibody (Fig. 5F) stained cytoplasmic vesicles and rare small circular structures that were also stained by the anti-cortactin antibody (Fig. 5G). In mCH5 cells, falloidin stained the cortical ring of Actin, cytosolic fibers and large circular structures (Fig. 5I). Such large circular structures were also stained by the anti-Rab7 (Fig. 5J) and by anti-cortactin (Fig. 5K) antibodies. Vertical Z-stack confocal acquisition of the same microscopic fields of the three examined clones showed that circular structures were located on the dorsal (apical) side of the cells (Fig. 5M, N, and O). Merge is shown in Figure 5 (D, H, and L). The large circular structures contained f-Actin and cortactin as is the case for CDRs (Buccione et al., 2004). We show here that over-expression of Rab7 may be considered a cause of CDRs genesis. The number of CDRs was more abundant in mCh5 cells, as assessed by blind observation of three different investigators: in Rab7 over-expressing cells, we observed CDRs in approximately 10% of the cell population, some of which (61%) showed co-localization of Rab7 with cortactin and f-Actin.

In FRT cells Rab7 activation is cAMP-dependent

Database screening (with MATINSPECTOR) (Croizet-Berger et al., 2002) (and with Pscan: http://159.149.160.51/pscan/) identified a potential cAMP response element in the promoter of the Rab7 gene. FRT cells have a normal adenylate cyclase complex sensitive to the diterpene activator Forskolin (Kohn et al., 1986; Akamizu et al., 1990). It has been shown that in autonomous thyroid adenomas, in which the cAMP cascade is constitutively activated, the expression of Rab5 and Rab7, but not Rab8, is increased and a higher proportion of Rab5 and Rab7 is membrane associated to promote Tg endocytosis (Croizet-Berger et al., 2002). To mimic autonomous thyroid adenoma conditions, we treated FRT cells with 10 μM Forskolin + 0.001M 3-Isobutyl-1-methylxanthine (IBMX) (inhibitor of cAMP and cGMP phosphodiesterases) and/or with 100 μM 8Br-cAMP (a membrane permeant cyclic AMP analog) + 0.001M IBMX for 96 h as described (Croizet-Berger et al., 2002), and we searched by WB with specific anti-Rab7, -Rab5, and -Rab8 antibodies in total cell lysates or in the Triton-X 100 (TX-100) soluble or insoluble fraction to detect the

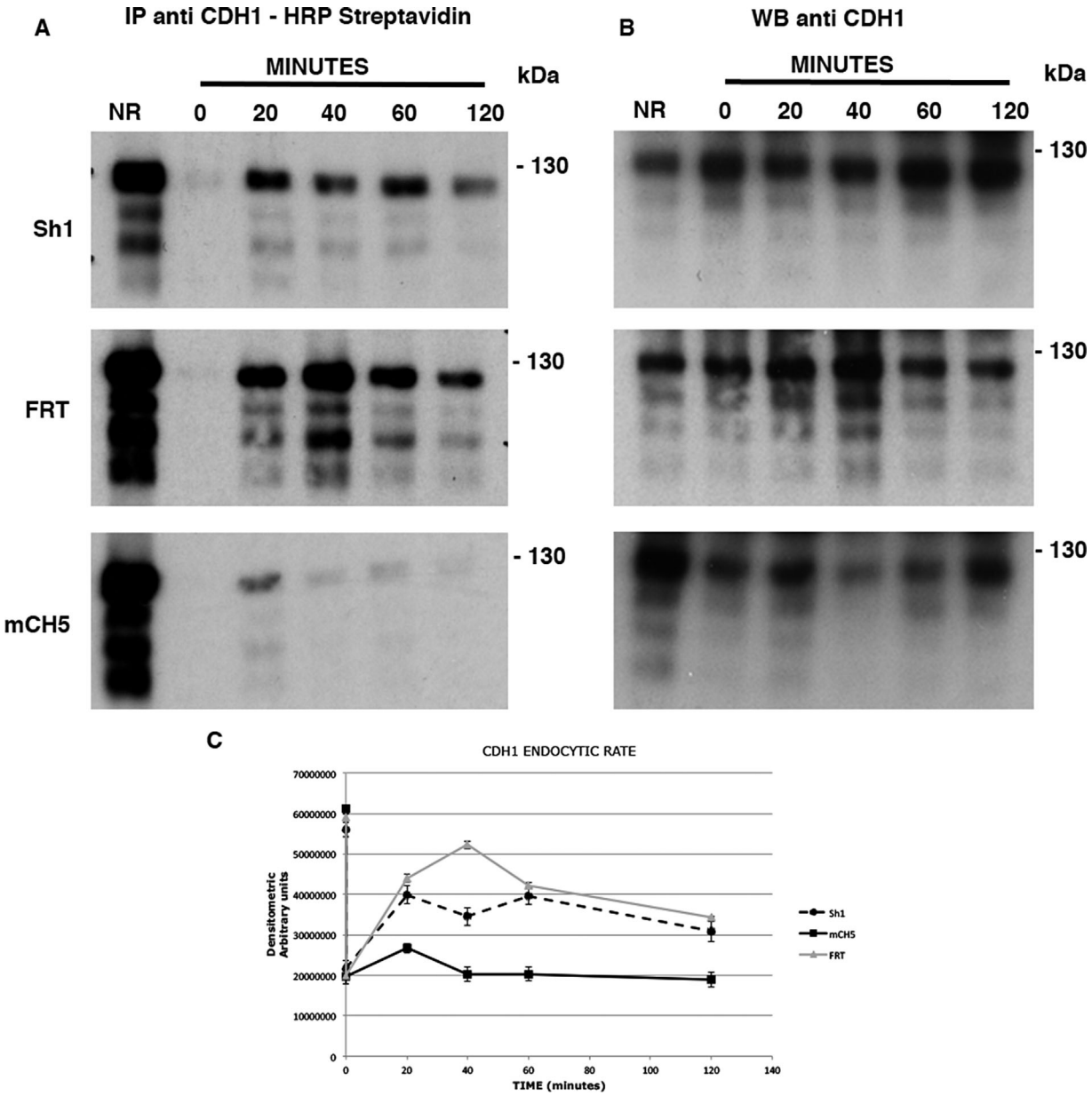

Fig. 3. Rab7 expression modulates CDH1 endocytosis. Endocytosis assay (see Materials and Methods) of immunoprecipitated CDH1 protein in Sh1, FRT, and mCH5 cells. A: at steady state, biotinylated CDH1, detected by HRP-conjugated streptavidin, was endocytosed by Sh1 and FRT cells but not by mCH5 cells. B: As loading control, after stripping, to detect the total immunoprecipitated CDH1, the same filters were re-probed with monoclonal antibodies anti CDH1. C: densitometric measurements of resolved bands (±SD) showed that endocytosis of CDH1 occurred with minor kinetic differences in Sh1 and FRT cells and was almost abolished in mCH5 cells. The reduction of CDH1 endocytosis rate in mCH5 cells was statistically significant ($P < 0.01$) at 20, 40, 60, and 120 min. *P*-values express statistical significance for mCH5 versus FRT comparisons.

membrane bound/active form of Rab7 (Chavrier et al., 1991; Rak et al., 2003, 2004; Cabrera et al., 2014). Stimulation with Forskolin or 8Br-cAMP does not significantly modify the total amount of Rab7, Rab5 and Rab8 in total cell lysates (Fig. 6A). FRT cell lysates were subjected to differential centrifugation to separate the soluble and the TX-100 insoluble membrane enriched compartment (Brown and Rose, 1992; Lichtenberg et al., 2013). In the TX-100 soluble fraction, we did not observe significant variations of Rab7 expression in cells stimulated or unstimulated with either Forskolin or 8Br-cAMP. In the TX-100 insoluble fraction, however, we found that the amount of membrane associated/active form of Rab7 was more than doubled when cells were stimulated with either Forskolin or 8Br-cAMP. No effect on Rab5 and little modification on Rab8 activity were detected (Fig. 6A). Rab7 normalized densitometric quantitation of WB signals is shown in Figure 6B.

We also quantified Rab7 mRNA expression by qRT-PCR in unstimulated and "chronic" Forskolin stimulated FRT and mCH5 cells. In FRT cells Forskolin stimulation led to a 50% increase of Rab7 mRNA transcript that was comparable to

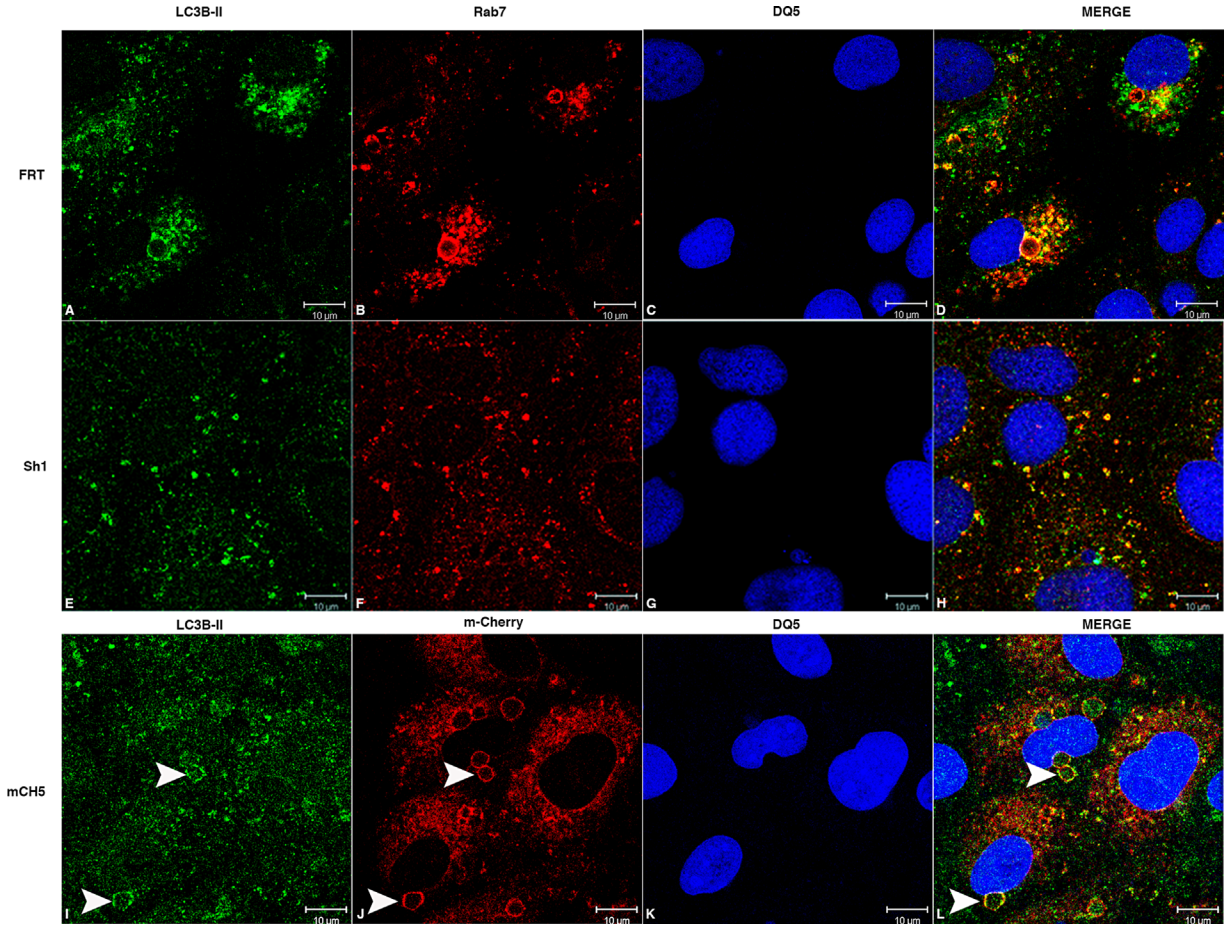

Fig. 4. Rab7 over-expression leads to mature autophagosomes genesis. Triple immunofluorescence staining with rabbit polyclonal anti-LC3B-II antibodies (A, E, I) and with mouse monoclonal anti-Rab7 antibodies (B, F) or Rab7-mCherry autofluorescence (J). DQ5 nuclear staining (C, G, K) and Merge (D, H, L) are shown. In FRT cells, LC3B-II and Rab7 were in part co-localized on small vesicles and on rare circular structure (A–D). In Sh1 cells, LC3B-II and Rab7 proteins were co-localized too; small vesicles were visible, but large circular structures were not present (E–H). In mCH5 clones over-expressing Rab7, we had a different context: in addition to being co-localized in the vesicular compartment, LC3B-II and Rab7 antibodies stained numerous large circular structures. Only some of them (white arrowheads) were LC3B-II and Rab7 mCherry positive (I, J, L). Images are representative of at least five different experiments.

Rab7 expression in mCH5 over-expressing cells. On the contrary, mCH5 cells were unresponsive to Forskolin stimulation: Rab7 transcription was reduced by 10–15% after stimulation (Fig. 6C).

In FRT cells PAK1 phosphorylation is enhanced after cAMP stimulation

We determined that in FRT cells, adenylate cyclase activation led to an increased amount of membrane bound Rab7. In mCH5 cells, Rab7 over-expression modulated Rac1 expression and activity as detected by PAK^{T423} phosphorylation. We wondered whether PAK^{T423} phosphorylation could be modified after cAMP stimulation in FRT cells. Therefore, FRT cells were stimulated with 10 µM Forskolin + 1 mM IBMX and/or with 100 µM 8Br-cAMP + 0.001M IBMX for 96 h (Croizet-Berger et al., 2002). After SDS PAGE of cell lysates and WB with the specific mouse monoclonal anti-Phospho-PAK T^{423} antibody, the densitometric evaluation (α-tubulin normalized) of resolved bands showed that after cAMP stimulation PAK^{T423} phosphorylation increased by 20% in FRT cells (Fig. 7).

CDH1 endocytosis is inhibited by cAMP stimulation in FRT cells

Rab7 over-expression in mCH5 cells led to a Rac1/PAK1 activation that in turn blocked CDH1 endocytosis. In FRT cells, cAMP stimulation led to increased Rab7 gene transcription, protein activation and PAK^{T423} phosphorylation. To close the circle and reconstitute in FRT cells what happened in mCH5 cells, we questioned whether cAMP stimulation could affect CDH1 endocytosis of fully polarized FRT cells. FRT cells grown on filters in bicameral systems were stimulated for 96 h with 10 µM Forskolin + 0.001M IBMX, and subjected to the endocytosis assay, as described by (Graeve et al., 1989). Cellular lysates were immunoprecipitated with monoclonal anti-CDH1 antibodies. After SDS PAGE and blotting onto nitrocellulose filter, biotinylated endocytosed CDH1 was detected with Streptavidin-HRP. As a loading control, the same filter, after stripping, was treated for WB with anti-CDH1 antibodies. Results show that FRT cells are able to endocytose CDH1 with the same kinetics as in Figure 4. CDH1 endocytosis was greatly inhibited after cAMP stimulation mimicking the behavior of mCH5 cells over-expressing Rab7. It is noteworthy that Forskolin stimulated cells expressed less CDH1 on plasma

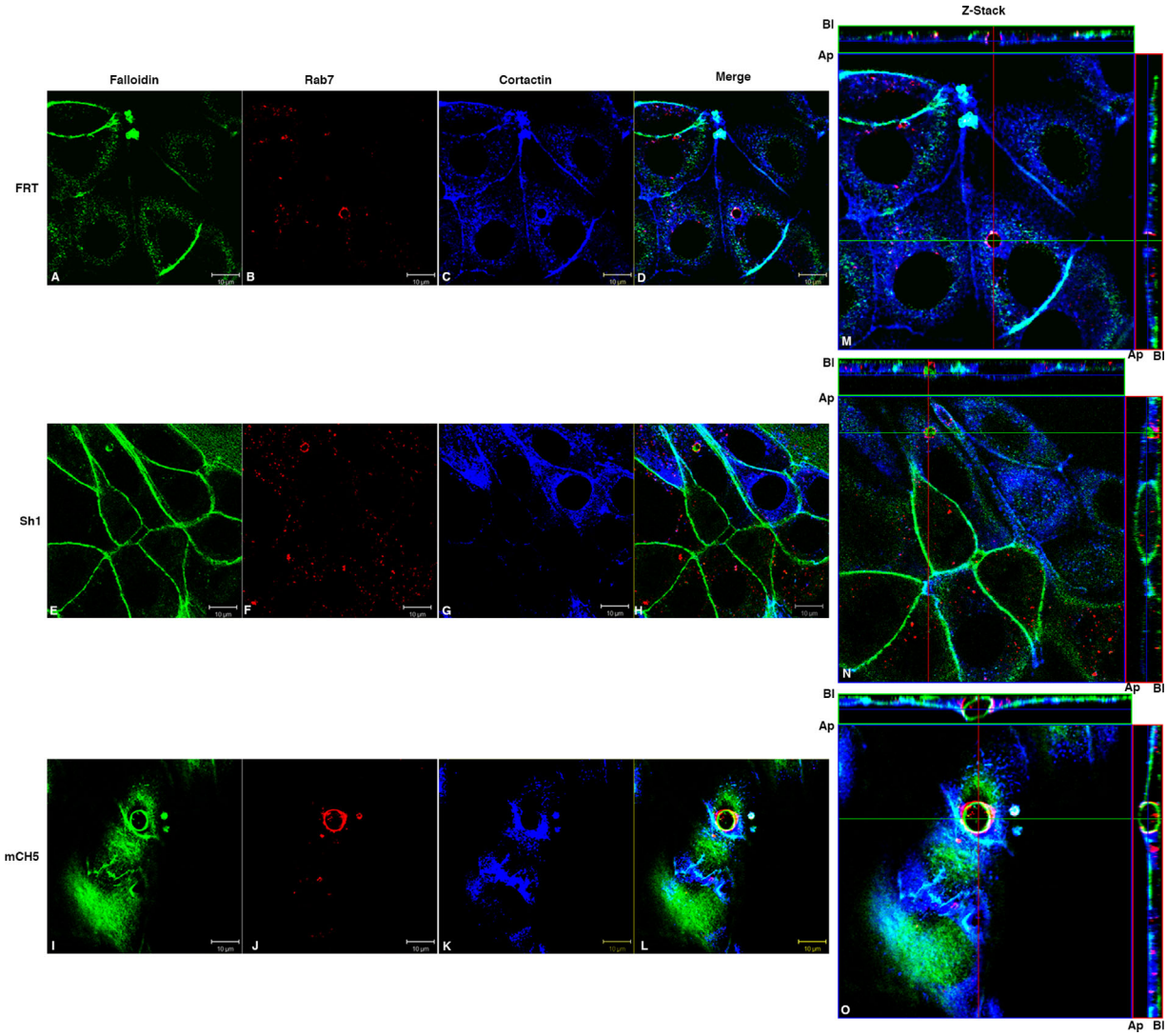

Fig. 5. Rab7 over-expression induces circular dorsal ruffles genesis. Triple immunofluorescence staining with falloidin Alexa fluor 488 conjugated (A, E, I) mouse monoclonal anti-Rab7 (B, F) or Rab7-mCherry autofluorescence (J) and rabbit polyclonal anti-cortactin antibodies (C, G, K). Merge is shown in (D, H, L). On the apical side of FRT and Sh1 cells, falloidin Alexa fluor 488 conjugated stained cortical actin and small circular structures (A, E) that were also stained by anti Rab7 (B, F) and anti cortactin (C, G) antibodies. On mCH5 cells, falloidin Alexa fluor 488 conjugated stained cortical actin, network of actin microfilaments and large circular structures that were also stained by Rab7-mCherry (J) and anti-cortactin (K) antibodies. Orthogonal projections of z-stack acquisition showed that these structures were indeed present on the apical side of the polarized cells (M–O). Ap: apical; Bl: basolateral. Images are representative of at least three different experiments.

membrane than unstimulated cells but certainly in sufficient amounts to be endocytosed (Fig. 8A). Densitometric analysis of the CDH1 endocytic rate is also shown (Fig. 8B).

Thyroglobulin pinocytosis occurs via CDRs in FRT and in mCH5 cells

In the thyroid gland, thyroglobulin (Tg) is secreted at the apical pole of thyrocytes into the colloid as macromolecular thyroid hormone precursor. Tg uptake, at the apical membrane of the thyroid cells, occurs mainly by pinocytosis, which can result from both fluid-phase pinocytosis or receptor-mediated endocytosis, although this last mechanism has never been formally proven. Tg then goes to the lysosomes, where it is believed to be degraded with the release of free T3 and T4 thyroid hormones (Marino and McCluskey, 2000). It has been shown that Tg endocytosis can be regulated by the expression or function of Rab5 and Rab7 and that in autonomous thyroid adenomas, where the cAMP pathway is constitutively activated, expression of Rab5 and Rab7 protein is increased (Croizet-Berger et al., 2002). We investigated how Tg endocytosis occurred in undifferentiated thyroid FRT cells and in mCH5 cell over-expressing Rab7. The FRT-L5 rat differentiated thyroid cells (Ambesi-Impiombato et al., 1980), capable of synthesizing and secreting Tg, were cultured for 48h. FRT-L5-conditioned culture media were collected, centrifuged and added to FRT and mCH5 cells growing on 35 mm plastic dishes and on 12 mm glass coverslips for different times. After 0, 20, 40 60, 120, 240, and 360 min and overnight (O/N), cells growing on glass cover slips were fixed and stained by double immunofluorescence with anti-Tg and anti-Rab7 antibodies. Cells growing on dishes were lysed and SDS–PAGE and WB with antibodies against Tg

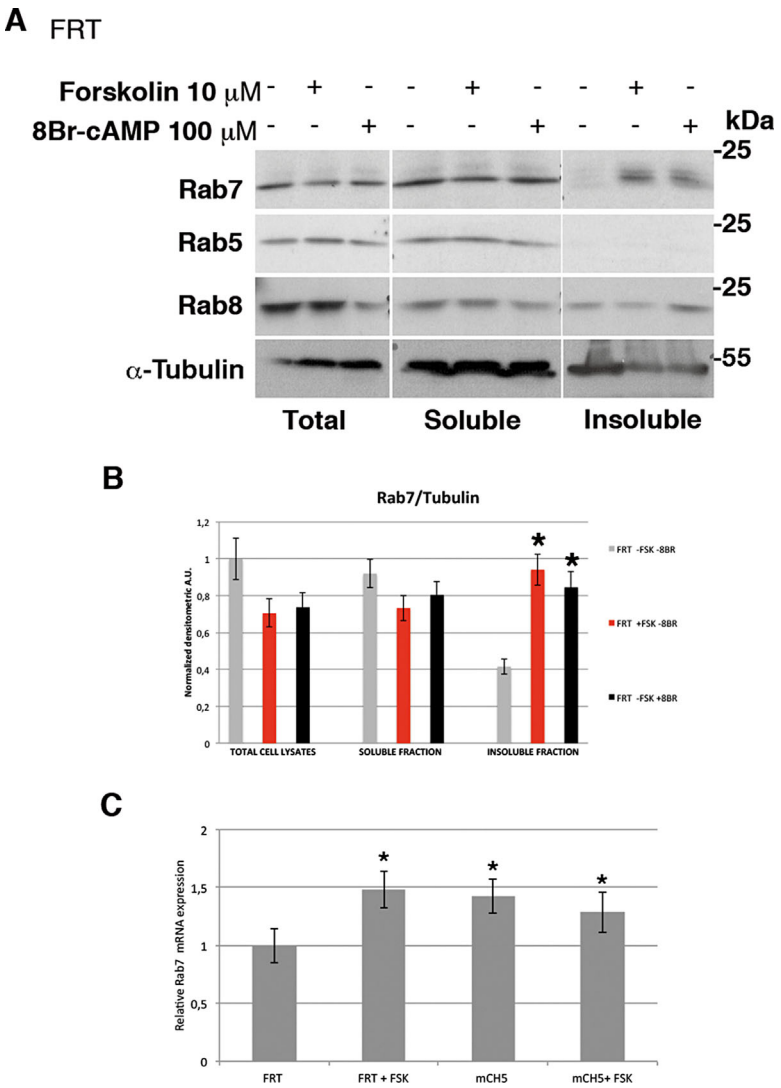

Fig. 6. In FRT cells Rab7 activation is cAMP-dependent. WB of cell lysates of FRT cells chronically stimulated (96 h) with 10 μM Forskolin or 100 μM 8Br-cAMP in presence of 0.001M IBMX with mouse monoclonal antibodies anti Rab7 and after stripping with rabbit polyclonal anti Rab5, mouse monoclonal anti Rab8 and as loading control with mouse monoclonal anti-α-tubulin. Stimulations with Forskolin or 8Br-cAMP did not modify the amount of Rab7, Rab5, and Rab8 proteins in total cell lysates (A). After differential centrifugation to isolate the TX-100 insoluble membranes-enriched compartment, in the soluble fraction there were no significant variations in Rab7 expression in FRT cells stimulated or not with Forskolin or 8Br-cAMP. In the insoluble fraction, conversely, we found that the amount of membrane associated/active form of Rab7 was more than double in Forskolin or 8Br-cAMP-stimulated cells with respect to the unstimulated cells. No effect on Rab5 and little modification on Rab8 activity were detected. α-tubulin normalized densitometric measurement of resolved bands (±SD) is shown (B). $^{*}P < 0.05$. *P*-values express statistical significance for insoluble fraction in Forskolin or 8Br-cAMP stimulated versus unstimulated FRT comparisons. C: Quantitative RT-PCR analysis was performed on FRT and mCH5 cells stimulated or not with Forskolin. The fold-change values indicate the relative change in the expression levels between FRT unstimulated cells and the other samples, assuming FRT cells as calibrator. Rab7 mRNA transcript was up regulated in the FRT cells after Forskolin stimulation. In mCH5 cells, as expected, Rab7 mRNA transcripts were significantly up-regulated, but decreased after Forskolin stimulation. Values represent the average determination ± SEM for three samples for each experimental condition carried out in triplicate. $^{*}P < 0.05$. P-values express statistical significance for each condition versus unstimulated FRT cells.

were performed. In FRT cells, IF with the anti-Rab7 antibody stained a vesicular compartment at all times analyzed; the anti-Tg antibody stained dense, large structures on the apical side of some cells after incubation with FRTL-5 Tg/containing, conditioned medium, particularly at the 120 and 240 min time points. Such large circular structures were well visible in vertical z-stack and orthogonal projections of confocal acquisitions (Fig. 9A (120 and 240 min)). WB analysis with anti Tg antibodies, provided similar results: in FRT cell lysates, exogenous Tg was visualized after 120–240 min (Fig. 9B).

mCH5 cells incubated with FRT-L5 conditioned medium gave different results both by IF and confocal microscopy and by WB analysis. If staining with anti Tg antibodies showed that Tg endocytosis occurred earlier than in FRT cells: it started after 20 min of incubation with FRT-L5 conditioned medium and lasted up to 360 min. Tg filled and Rab7 stained CDRs, were clearly visible in vertical z-stack and orthogonal projections of confocal acquisitions at 20, 40, 60, 120, and 240 min. After 18 h of incubation (O/N), Rab7 positive CDRs were visible but no Tg staining was detectable (Fig. 9C). WB on cell lysates with

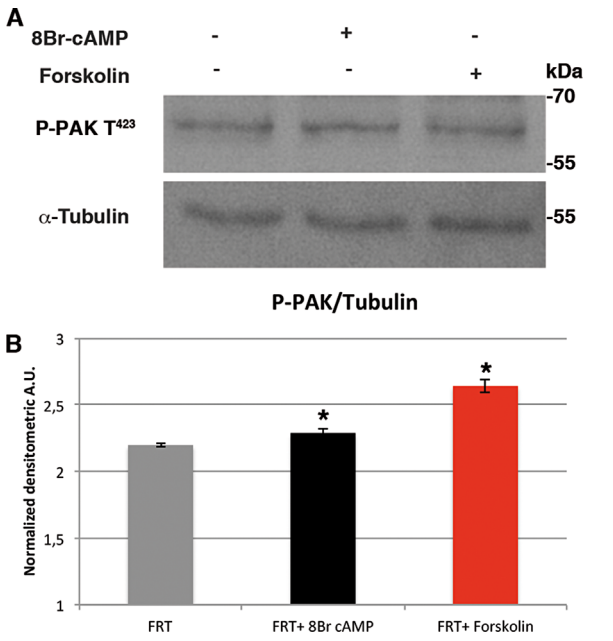

Fig. 7. In FRT cells PAK1 phosphorylation is enhanced after cAMP stimulation. A: WB of FRT cell lysates chronically stimulated (96 h) with 10 μM Forskolin or with or 100 μM 8Br-cAMP in the presence of 0.001M IBMX with rabbit polyclonal antibodies anti-PAK p-T^{423} and after stripping, with monoclonal antibodies anti α-tubulin. In FRT cells, Forskolin stimulation increased PAK1 phosphorylation by about 20%, as shown in densitometric measurements (α-tubulin normalized (±SD) B. $^{*}P < 0.01$. *P*-values express statistical significance for stimulated versus unstimulated FRT comparisons.

anti-Tg antibodies was in good agreement with IF results (Fig. 9D). As shown in the densitometric analysis of the WB results, endocytosis of exogenous Tg starts after 120 min and lasts until 240 min in FRT cells. In mCH5 cell Tg endocytosis starts at 20 min, peaks at 60 min and can be detected up to 360 min of incubation with FRT-L5 conditioned medium (Fig. 9E). FRT-L5 conditioned medium was loaded on SDS PAGE in the last (Fig. 9B) and in the first (Fig. 9D) lane as a control. As loading control, WB with anti-α-tubulin antibodies was performed. Tg pinocytosis was enhanced in Rab7 over-expressing mCH5 cells relative to parental FRT.

Discussion

Small GTPases belonging to the Rab and Rac family play a pivotal role in endocytosis and actin remodeling, respectively (Kjoller and Hall, 2001). Rab and Rac proteins are also involved in intracellular traffic and their intracellular localization is important for determining the site(s) at which their signaling occurs (Del Pozo and Schwartz, 2007). It has been shown that a molecular, functional (Frasa et al., 2010) and physical (Sun et al., 2005) interactions between Rab7 and Rac1 in CDH1 endocytosis and ruffled border formation exists. We present here data that firmly support the notion that a functional and molecular interaction between Rab7 and Rac1 also exists in thyroid cells. In a polarized epithelium, integrity of AJ is crucial to prevent epithelial cell migration. CDH1 is the main structural protein of the AJ and its endocytosis is Rac1-dependent and plays a major role in the remodeling of adhesive contacts (Palacios et al., 2001; Paterson et al., 2003). We were interested in determining the role of the Rab7, Rac1, and CDH1 axis in endocytosis in polarized epithelial cell lines.

In this work, we decided to use only two FRT transfected clones: one where Rab7 expression was up-regulated by more than 60%, and another in which Rab7 RNAi was efficient and

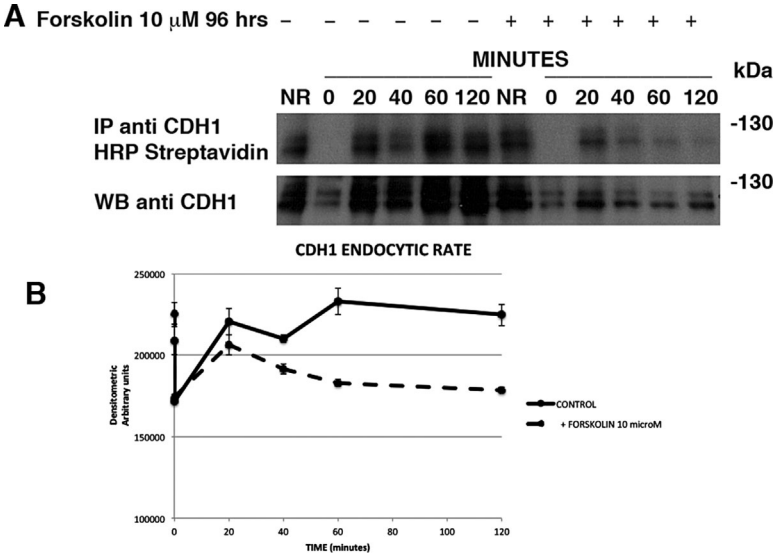

Fig. 8. CDH1 endocytosis is inhibited by cAMP stimulation in FRT cells. Endocytosis assay (see Materials and Methods) of immunoprecipitated CDH1, detected by HRP conjugated streptavidin, in FRT cells in basal condition or in cells chronically stimulated with 10 μM Forskolin in the presence of 0.001M IBMX. A: Biotinylated CDH1 was endocytosed by FRT cells. cAMP stimulation strongly inhibited CDH1 endocytosis. As a loading control, after stripping, to detect the total immunoprecipitated CDH1, the same filters were re-probed with monoclonal anti-CDH1 antibodies. B: Densitometric measurements of resolved bands (±SD) confirmed that CDH1 endocytosis was almost abolished after Forskolin stimulation. Reduction of CDH1 endocytosis rate after Forskolin stimulation was statistically significant ($P < 0.05$) at 20, 40, 60, and 120 min. *P*-values express statistical significance for unstimulated versus stimulated FRT comparisons.

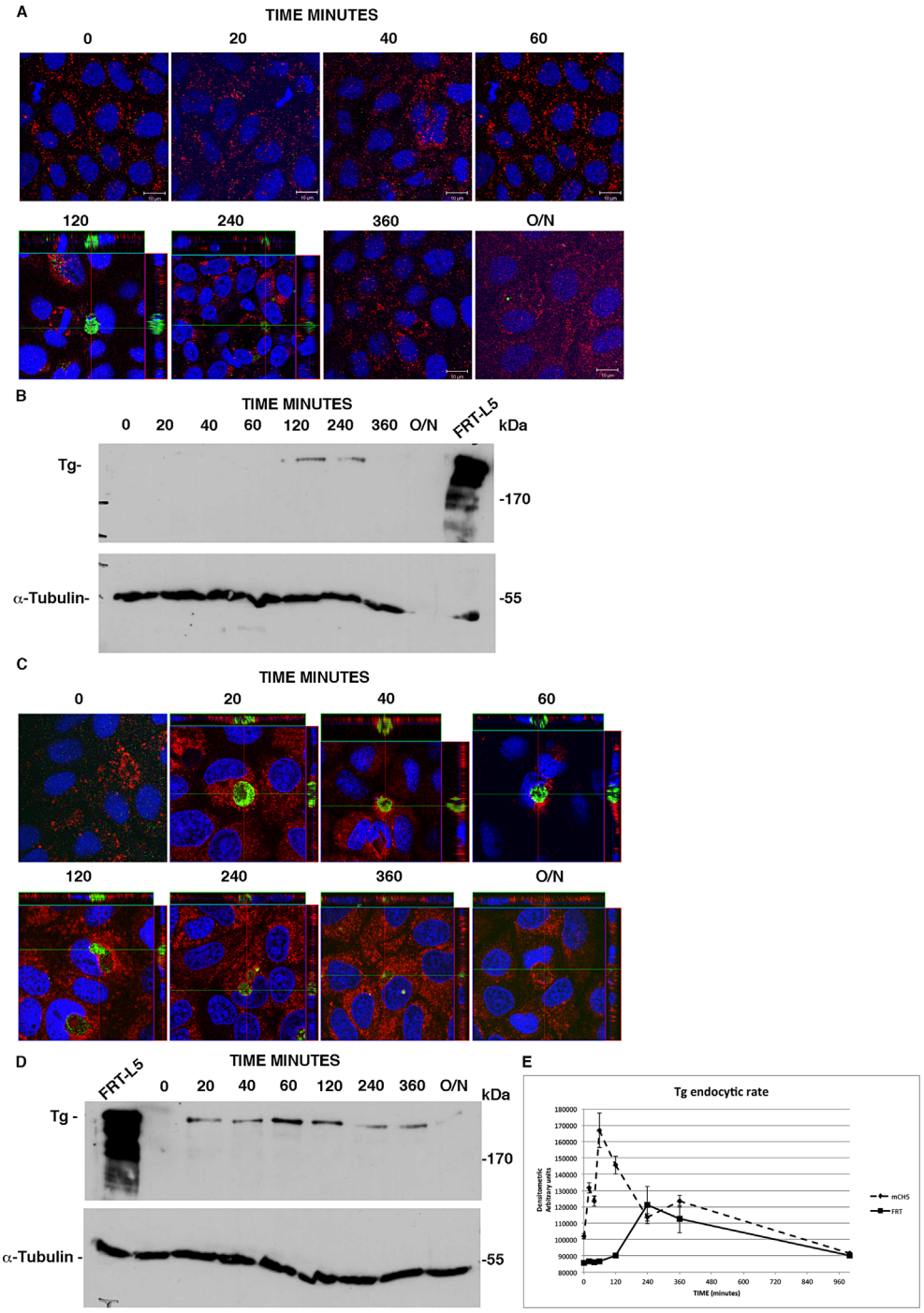

Fig. 9. Thyroglobulin pinocytosis occurs via CDRs in FRT and in mCH5 cells. Triple immunofluorescence staining with rabbit polyclonal antibodies anti Tg (green) and mouse monoclonal antibodies anti Rab7 (red), nuclei (blue) were counter stained with DQ5. Time course by immunofluorescence of exogenous Tg endocytosis in FRT (A: upper panel) and in mCH5 (C: lower panel) cells growing on glass coverslips in presence of FRT-L5 conditioned medium (Tg containing). In FRT cells, Tg staining (green) was detected in large circular structures, Rab7 stained (red) only after 120 and 240 min (A); in mCH5 cells (C), Tg staining (green) was detected early: it was visible already after 20 min and it lasted until 360 min. Tg staining was present in large circular structures facing on the apical side of the cells that were stained by Rab7 antibodies (red), as occurs in CDRs. To visualize CDRs in Tg pinocytosis, when present (A: 120 and 240 min; B from 20 min to O/N), confocal acquisitions were done along the z-axis and orthogonal projections are shown. WB results of cell lysates of FRT (B) and mCH5 (D) cells growing on plastic dishes, in presence of FRT-L5-conditioned medium (Tg containing), with rabbit polyclonal anti-Tg antibodies. As a control, in the last lane of panel B and in the first lane of panel D, FRT-L5 conditioned medium was loaded. In good agreement with immunofluorescence results, we show that mCH5 cells were able to endocytose exogenous Tg better than FRT cells. As loading control, WB with mouse monoclonal anti-α-tubulin antibodies is shown. Densitometric determination of the WB results (E) (±SD): in FRT cells endocytosis of exogenous Tg started after 120 min and lasted until 240 min. In mCH5 cells, Tg endocytosis started at 20 min, peaked at 60 min and lasted until 360 min of incubation with FRT-L5-conditioned medium. Differences in Tg endocytosis rate between FRT and mCH5 cells were statistically significant ($P < 0.05$) at 20, 40, 60, and 120 min. *P*-values express statistical significance for mCH5 versus FRT comparisons.

Rab7 protein expression was down-regulated by about 40% relative to control FRT cells. Another FRT Rab7 over-expressing clone (mCH8) was analyzed, in some experiments, and gave the same results as mCH5 (not shown).

We show here that Rab7 over-expression in mCH5 cells leads to Rac1 over-expression and activation measured as the phosphorylation of its effector PAK1. PAK1 was originally identified, along with other members of the PAK family of kinases, due to its ability to bind the active (GTP bound) form of the Rho-family GTPases, Cdc42, and Rac1 (Manser et al., 1994; Knaus et al., 1995). It was demonstrated that PAK1 binding to GTP-bound Rac1 results in an increase in kinase activity. PAK1 kinase functions as an effector of Rac1 (Lu and Mayer, 1999). Rac1 is involved in adherent junction stability and in CDH1 endocytosis. In human epidermal keratinocytes, Rac1 plays a complex role in adherent junction assembly and disassembly, dependent on both junctional maturity and cellular context (Braga et al., 1997, 1999; Akhtar et al., 2000). In MDCK cells, the expression of constitutively activated Rac1 results in increased accumulation of CDH1 at sites of cell–cell contact (Ridley et al., 1995; Takaishi et al., 1997). Tiam-1, GEF for Rac1, have been shown to localize to cell–cell contacts and prevent HGF-induced cell scattering of MDCK cells which is consistent with the observation that activated Rac1 increases CDH1–mediated cell adhesion (Hordijk et al., 1997). However, it has also been reported that in MDCK cells, HGF- mediated disruption of adherent junctions was inhibited by dominant negative Rac1 (Potempa and Ridley, 1998). It has been also demonstrated that CDH1 endocytosis is regulated by the activity state of CDH1 through the activation of the Rac/Cdc42- IQGAP1 system induced by CDH1 trans interaction (Izumi et al., 2004). CDH1 endocytosis, dependent by Rac1 activation or deactivation, can regulate both assembly and disassembly of adherent junctions. We investigated whether Rab7 over-expression dependent Rac1 activation could regulate CDH1 endocytosis in thyroid polarized epithelial cells. We determined that in FRT and in Sh1 cells, CDH1 endocytosis occurred with the same kinetics. CDH1 endocytosis in mCH5 cells was almost completely inhibited. This is not surprising: in other experimental systems Rac activation impairs CDH1 endocytosis (Izumi et al., 2004). FRT cells grown on filters are fully polarized with high TER and CDH1 dimers well engaged 'in trans' with cadherins of adjacent cells. In agreement with the observations of Izumi (Izumi et al., 2004), we think that Rac1 activation due to Rab7 over-expression leads to cytoskeletal reorganization through IQGAP-1 and impairs CDH1 trans-engaged endocytosis.

Rab7 is considered to regulate the biogenesis of late endosomes, lysosomes, phagosomes and autophagosomes (Progida et al., 2006; Hutagalung and Novick, 2011). The endocytic pathways and autophagy are closely linked.

There is evidence that large autophagosomes induced by Armus (a Rac effector) expression require late endocytic recycling, but not lysosomal fusion (Carroll et al., 2013). In mCH5 cells, Rab7 over-expression induces Rac1 activation and autophagosome accumulation.

To this purpose, we investigated the constitutive autophagocytic pathway in FRT and in under or over-expressing Rab7 transfected cells.

We focused on LC3B-II and Beclin 1 because of their principal role in autophagy (Levine and Deretic, 2007). Cellular events occurring in mCH5 cells, such as the increase in LC3B-II autophagosome membrane-associated isoform and Beclin-1 expression levels, were consistent with autophagy. IF experiments show that Rab7 and LC3B-II co-localize on the autophagosome membrane in FRT, Sh1, and mCH5 cells. The morphology of the mature autophagosome stained with anti LC3B-II and Rab7 antibodies, detected in mCH5 cells, was completely different from that of FRT and Sh1 resembling that of Circular Dorsal Ruffles (Hoon et al., 2012).

Was Rab7 over-expression sufficient to induce CDRs? We identified two different types of Rab7-positive large vacuolar structures in mCH5 cells in about 10% of the cell population: the first (39%) are also LC3B-II positive and were identified as mature autophagosomes, while the second (61%) were located in the apical domain in polarized cells, similarly to CDRs. In mCH5 cells, we identified large vacuolar structures that are positive for actin and cortactin immunostaining. It has been described that actin dynamic leading to CDRs genesis needs: Rac activation (Miki et al., 2000; Eden et al., 2002), PAK1 phosphorylation (Dharmawardhane et al., 2000) and downstream pathway expression of actin related protein such cortactin that has a predominant role in CDRs genesis (Buccione et al., 2004). These three events occur in FRT cells over-expressing Rab7. Other proteins related to endocytosis, such as dynamin (Orth and McNiven, 2003) and Rab5 (Zerial and McBride, 2001; Palamidessi et al., 2008), have been shown to participate in CDRs genesis. Using IF, we searched in mCH5 cells for Rab5 co-localization with Rab7 on CDRs and found that the anti-Rab5 antibodies give fine punctate staining that sometimes co-localized with Rab7 (transition phase early/late endosomes) (Rink et al., 2005; Poteryaev et al., 2010); rarely, CDRs were co-stained with anti-Rab7 and anti-Rab5 antibodies (Supplementary Fig. S2).

CDRs are multifunctional and dynamic structures: they appear and disappear within 5–20 min, they can form transiently at the site at which the growth factor is applied (Buccione et al., 2004; Palamidessi et al., 2008), it has been proposed that CDRs might promote the degradation of ECM during three-dimensional migration (Suetsugu et al., 2003) and they are sites of internalization events, such as fluid phase endocytosis (Buccione et al., 2004; Hasegawa et al., 2012). Database screening with MATINSPECTOR (Croizet-Berger et al., 2002) and with P-Scan identified a potential cAMP response element in the promoter of the Rab7 gene. FRT cells, although undifferentiated, have a normal adenylate cyclase complex sensitive to the diterpene activator Forskolin (Kohn et al., 1986; Akamizu et al., 1990). In FRT cells, we found that Forskolin stimulation caused an increase in the transcription of Rab7 mRNA. We investigated the expression level and membrane recruitment of Rab7 protein in cAMP stimulated FRT cells. In total cellular lysates of cAMP stimulated cells, we did not find any substantial differences in Rab7 expression. After differential centrifugation of TX-100 cell lysates to isolate soluble and insoluble fractions, a greater amount of Rab7 protein was found in the membranous compartments TX-100 insoluble/active fraction. Rab7 analysis by qRT-PCR on mCH5 cells showed that Rab7 mRNA transcripts were significantly up-regulated but decreased after Forskolin stimulation. We do not know exactly how to explain this phenomenon; we speculate that a possible down-regulation of Rab7 expression after Forskolin stimulation could be due to mRNA instability and degradation. Moreover, we know that IF analysis of Rab7-mCherry on mCH5 cells after Forskolin stimulation resulted in no staining (not shown).

In mCH5 cells, Rab7 over-expression modulated Rac1 expression and activity as detected by PAK^{T423} phosphorylation. Forskolin stimulation of FRT cells leads to increased phosphorylation of PAK^{T423}. This reminded us of the results from mCH5 cells over-expressing Rab7. We addressed the issue of CDH1 endocytosis in FRT cells stimulated with Forskolin: after cAMP pathway activation, CDH1 endocytosis was blocked similarly to that which was observed in mCH5 cells. We propose that Rab7 over-expression or over-activation increases Rac activation, which impairs CDH1 endocytosis, in agreement with previous studies (Izumi et al., 2004).

In autonomous thyroid adenomas, in which the cAMP cascade is constitutively activated, Rab5 and Rab7 expression, but not Rab8, is increased and a higher proportion of Rab5 and Rab7 is membrane associated (active) in order to promote Tg endocytosis (Croizet-Berger et al., 2002). Activation of the cAMP pathway with dibutyryl c-AMP or TSH has long been known to produce pseudopods and intracellular colloid droplets in dog thyroid slices (Pastan and Wollman, 1967). These authors noted that the droplets observed after incubation with dibutyryl c-AMP or TSH must be newly formed, since they were not present before the addition of these substances and many occurred on the apical ends of cells in configurations characteristic of newly formed droplets. Colloid droplets resemble what we today define as CDRs.

We found that the Rab7 over-expressing cells were able to endocytose exogenous thyroglobulin via macropinosome/CDRs better than control cells. We suggest that the increased thyroglobulin endocytosis found in thyroid autonomous adenomas due to Rab7 increased expression may occur via CDRs.

Acknowledgments

This work was supported by a grant from Ministero dell'Istruzione, dell'Universita` e della Ricerca PRIN 2012 to L.N. and C.B. and partially supported by AIRC (grant IG2013 N.14709 to C.B.). We thank Prof. Antonio Porcellini and Dr. Daria Monti (University "Federico II," Napoli) for their helpful discussion and Prof. Giuseppe Matarese (University "Federico II," Napoli) for having continuously supported this paper. We thank Sig. Mario Senesi (Department of Molecular Medicine and Medical Biotechnologies University "Federico II," Napoli) for technical support.

Literature Cited

Akamizu T, Ikuyama S, Saji M, Kosugi S, Kozak C, McBride OW, Kohn LD. 1990. Cloning, chromosomal assignment, and regulation of the rat thyrotropin receptor: Expression of the gene is regulated by thyrotropin, agents that increase cAMP levels, and thyroid autoantibodies. Proc Natl Acad Sci USA 87:5677–5681.
Akhtar N, Hotchin NA. 2001. RAC1 regulates adherens junctions through endocytosis of E-cadherin. Mol Biol Cell 12:847–862.
Akhtar N, Hudson KR, Hotchin NA. 2000. Co-localization of Rac1 and E-cadherin in human epidermal keratinocytes. Cell Adhes Commun 7:465–476.
Ambesi-Impiombato FS, Parks LA, Coon HG. 1980. Culture of hormone-dependent functional epithelial cells from rat thyroids. Proc Natl Acad Sci USA 77:3455–3459.
Bokoch GM. 2003. Biology of the p21-activated kinases. Annu Rev Biochem 72:743–781.
Braga VM, Del Maschio A, Machesky L, Dejana E. 1999. Regulation of cadherin function by Rho and Rac: Modulation by junction maturation and cellular context. Mol Biol Cell 10:9–22.
Braga VM, Machesky LM, Hall A, Hotchin NA. 1997. The small GTPases Rho and Rac are required for the establishment of cadherin-dependent cell-cell contacts. J Cell Biol 137:1421–1431.
Bretscher MS, Lutter R. 1988. A new method for detecting endocytosed proteins. EMBO J 7:4087–4092.
Brown DA, Rose JK. 1992. Sorting of GPI-anchored proteins to glycolipid-enriched membrane subdomains during transport to the apical cell surface. Cell 68:533–544.
Bryant DM, Stow JL. 2004. The ins and outs of E-cadherin trafficking. Trends Cell Biol 14:427–434.
Bucci C, Frunzio R, Chiariotti L, Brown AL, Rechler MM, Bruni CB. 1988. A new member of the ras gene superfamily identified in a rat liver cell line. Nucleic Acids Res 16:9979–9993.
Bucci C, Thomsen P, Nicoziani P, McCarthy J, van Deurs B. 2000. Rab7: A key to lysosome biogenesis. Mol Biol Cell 11:467–480.
Buccione R, Orth JD, McNiven MA. 2004. Foot and mouth: Podosomes, invadopodia and circular dorsal ruffles. Nat Rev Mol Cell Biol 5:647–657.
Cabrera M, Nordmann M, Perz A, Schmedt D, Gerondopoulos A, Barr F, Piehler J, Engelbrecht-Vandre S, Ungermann C. 2014. The Mon1-Ccz1 GEF activates the Rab7 GTPase Ypt7 via a longin-fold-Rab interface and association with PI3P-positive membranes. J Cell Sci 127:1043–1051.
Cali G, Gentile F, Mogavero S, Pallante P, Nitsch R, Ciancia G, Ferraro A, Fusco A, Nitsch L. 2012. CDH16/Ksp-cadherin is expressed in the developing thyroid gland and is strongly down-regulated in thyroid carcinomas. Endocrinology 153:522–534.
Cali G, Retta SF, Negri R, Damiano I, Gentile R, Tarone G, Nitsch L, Garbi C. 1998. Beta1B integrin interferes with matrix assembly but not with confluent monolayer polarity, and alters some morphogenetic properties of FRT epithelial cells. Eur J Cell Biol 75:107–117.
Cali G, Zannini M, Rubini P, Tacchetti C, D'Andrea B, Affuso A, Wintermantel T, Boussadia O, Terracciano D, Silberschmidt D, Amendola E, De Felice M, Schutz G, Kemler R, Di Lauro R, Nitsch L. 2007. Conditional inactivation of the E-cadherin gene in thyroid follicular cells affects gland development but does not impair junction formation. Endocrinology 148:2737–2746.
Carroll B, Mohd-Naim N, Maximiano F, Frasa MA, McCormack J, Finelli M, Thoresen SB, Perdios L, Daigaku R, Francis RE, Futter C, Dikic I, Braga VM. 2013. The TBC/RabGAP Armus coordinates Rac1 and Rab7 functions during autophagy. Dev Cell 25:15–28.
Chavrier P, Gorvel JP, Stelzer E, Simons K, Gruenberg J, Zerial M. 1991. Hypervariable C-terminal domain of rab proteins acts as a targeting signal. Nature 353:769–772.
Christoforidis S, McBride HM, Burgoyne RD, Zerial M. 1999. The Rab5 effector EEA1 is a core component of endosome docking. Nature 397:621–625.
Croizet-Berger K, Daumerie C, Couvreur M, Courtoy PJ, van den Hove MF. 2002. The endocytic catalysts, Rab5a, and Rab7, are tandem regulators of thyroid hormone production. Proc Natl Acad Sci USA 99:8277–8282.
del Pozo MA, Price LS, Alderson NB, Ren XD, Schwartz MA. 2000. Adhesion to the extracellular matrix regulates the coupling of the small GTPase Rac to its effector PAK. EMBO J 19:2008–2014.
Del Pozo MA, Schwartz MA. 2007. Rac, membrane heterogeneity, caveolin, and regulation of growth by integrins. Trends Cell Biol 17:246–250.
Dharmawardhane S, Schurmann A, Sells MA, Chernoff J, Schmid SL, Bokoch GM. 2000. Regulation of macropinocytosis by p21-activated kinase-1. Mol Biol Cell 11:3341–3352.
Eden S, Rohatgi R, Podtelejnikov AV, Mann M, Kirschner MW. 2002. Mechanism of regulation of WAVE1-induced actin nucleation by Rac1 and Nck. Nature 418:790–793.
Edinger AL, Cinalli RM, Thompson CB. 2003. Rab7 prevents growth factor-independent survival by inhibiting cell-autonomous nutrient transporter expression. Dev Cell 5:571–582.
Frasa MA, Maximiano FC, Smolarczyk K, Francis RE, Betson ME, Lozano E, Goldenring J, Seabra MC, Rak A, Ahmadian MR, Braga VM. 2010. Armus is a Rac1 effector that inactivates Rab7 and regulates E-cadherin degradation. Curr Biol 20:198–208.
Graeve L, Drickamer K, Rodriguez-Boulan E. 1989. Polarized endocytosis by –Darby canine kidney cells transfected with functional chicken liver glycoprotein receptor. J Cell Biol 109:2809–2816.
Harrison RE, Bucci C, Vieira OV, Schroer TA, Grinstein S. 2003. Phagosomes fuse with late endosomes and/or lysosomes by extension of membrane protrusions along microtubules: Role of Rab7 and RILP. Mol Cell Biol 23:6494–6506.
Hasegawa J, Tsujita K, Takenawa T, Itoh T. 2012. ARAP1 regulates the ring size of circular dorsal ruffles through Arf1 and Arf5. Mol Biol Cell 23:2481–2489.
Hoon JL, Wong WK, Koh CG. 2012. Functions and regulation of circular dorsal ruffles. Mol Cell Biol 32:4246–4257.
Hordijk PL, ten Klooster JP, van der Kammen RA, Michiels F, Oomen LC, Collard JG. 1997. Inhibition of invasion of epithelial cells by Tiam1-Rac signaling. Science 278:1464–1466.
Hutagalung AH, Novick PJ. 2011. Role of Rab GTPases in membrane traffic and cell physiology. Physiolo Rev 91:119–149.
Izumi G, Sakisaka T, Baba T, Tanaka S, Morimoto K, Takai Y. 2004. Endocytosis of E-cadherin regulated by Rac and Cdc42 small G proteins through IQGAP1 and actin filaments. J Cell Biol 166:237–248.
Jaffe AB, Hall A. 2005. Rho GTPases: Biochemistry and biology. Annu Rev Cell Dev Biol 21:247–269.
Jager S, Bucci C, Tanida I, Ueno T, Kominami E, Saftig P, Eskelinen EL. 2004. Role for Rab7 in maturation of late autophagic vacuoles. J Cell Sci 117:4837–4848.
Kang R, Zeh HJ, Lotze MT, Tang D. 2011. The Beclin 1 network regulates autophagy and apoptosis. Cell Death Differ 18:571–580.
Kjoller L, Hall A. 2001. Rac mediates cytoskeletal rearrangements and increased cell motility induced by urokinase-type plasminogen activator receptor binding to vitronectin. Journal Cell Biol 152:1145–1157.
Knaus UG, Morris S, Dong HJ, Chernoff J, Bokoch GM. 1995. Regulation of human leukocyte p21-activated kinases through G protein–coupled receptors. Science 269:221–223.
Kohn LD, Alvarez F, Marcocci C, Kohn AD, Corda D, Hoffman WE, Tombaccini D, Valente WA, de Luca M, Santisteban P, Grollman EF. 1986. Monoclonal antibody studies defining the origin and properties of autoantibodies in Graves' disease. Ann NY Acad Sci 475:157–173.
Krueger EW, Orth JD, Cao H, McNiven MA. 2003. A dynamin-cortactin-Arp2/3 complex mediates actin reorganization in growth factor-stimulated cells. Mol Biol Cell 14:1085–1096.
Levine B, Deretic V. 2007. Unveiling the roles of autophagy in innate and adaptive immunity. Nat Rev Immunol 7:767–777.
Lichtenberg D, Ahyayauch H, Alonso A, Goni FM. 2013. Detergent solubilization of lipid bilayers: A balance of driving forces. Trends Biochem Sci 38:85–93.
Lozano E, Betson M, Braga VM. 2003. Tumor progression: Small GTPases and loss of cell-cell adhesion. BioEssays 25:452–463.
Lu W, Mayer BJ. 1999. Mechanism of activation of PAK1 kinase by membrane localization. Oncogene 18:797–806.
Machesky LM, Hall A. 1997. Role of actin polymerization and adhesion to extracellular matrix in Rac- and Rho-induced cytoskeletal reorganization. J Cell Biol 138:913–926.
Manser E, Leung T, Salihuddin H, Zhao ZS, Lim L. 1994. A brain serine/threonine protein kinase activated by Cdc42 and Rac1. Nature 367:40–46.
Marino M, McCluskey RT. 2000. Role of thyroglobulin endocytic pathways in the control of thyroid hormone release. Am J Physiol Cell Physiol 279:C1295–C1306.
Mascia A, De Felice M, Lipardi C, Gentile R, Cali G, Zannini M, Di Lauro R, Nitsch L. 1997. Transfection of TTF-1 gene induces thyroglobulin gene expression in undifferentiated FRT cells. Biochim Biophys Acta 1354:171–181.
Miki H, Yamaguchi H, Suetsugu S, Takenawa T. 2000. IRSp53 is an essential intermediate between Rac and WAVE in the regulation of membrane ruffling. Nature 408:732–735.
Orth JD, Krueger EW, Weller SG, McNiven MA. 2006. A novel endocytic mechanism of epidermal growth factor receptor sequestration and internalization. Cancer Res 66:3603–3610.
Orth JD, McNiven MA. 2003. Dynamin at the actin-membrane interface. Curr Opin Cell Biol 15:31–39.
Palacios F, Price L, Schweitzer J, Collard JG, D'Souza-Schorey C. 2001. An essential role for ARF6-regulated membrane traffic in adherens junction turnover and epithelial cell migration. EMBO J 20:4973–4986.
Palamidessi A, Frittoli E, Garre M, Faretta M, Mione M, Testa I, Diaspro A, Lanzetti L, Scita G, Di Fiore PP. 2008. Endocytic trafficking of Rac is required for the spatial restriction of signaling in cell migration. Cell 134:135–147.
Pastan I, Wollman SH. 1967. Colloid droplet formation in dog thyroid in vitro. Induction by dibutyrl cyclic-AMP. J Cell Biol 35:262–266.
Paterson AD, Parton RG, Ferguson C, Stow JL, Yap AS. 2003. Characterization of E-cadherin endocytosis in isolated MCF-7 and chinese hamster ovary cells: The initial fate of unbound E-cadherin. J Biol Chem 278:21050–21057.
Potempa S, Ridley AJ. 1998. Activation of both MAP kinase and phosphatidylinositide 3-kinase by Ras is required for hepatocyte growth factor/scatter factor-induced adherens junction disassembly. Mol Biol Cell 9:2185–2200.
Poteryaev D, Datta S, Ackema K, Zerial M, Spang A. 2010. Identification of the switch in early-to-late endosome transition. Cell 141:497–508.
Progida C, Spinosa MR, De Luca A, Bucci C. 2006. RILP interacts with the VPS22 component of the ESCRT-II complex. Biochem Biophys Res Commun 347:1074–1079.

Rak A, Pylypenko O, Durek T, Watzke A, Kushnir S, Brunsveld L, Waldmann H, Goody RS, Alexandrov K. 2003. Structure of Rab GDP-dissociation inhibitor in complex with prenylated YPT1 GTPase. Science 302:646–650.
Rak A, Pylypenko O, Niculae A, Pyatkov K, Goody RS, Alexandrov K. 2004. Structure of the Rab7:REP-1 complex: Insights into the mechanism of Rab prenylation and choroideremia disease. Cell 117:749–760.
Ridley AJ, Comoglio PM, Hall A. 1995. Regulation of scatter factor/hepatocyte growth factor responses by Ras, Rac, and Rho in MDCK cells. Mol Cell Biol 15:1110–1122.
Rink J, Ghigo E, Kalaidzidis Y, Zerial M. 2005. Rab conversion as a mechanism of progression from early to late endosomes. Cell 122:735–749.
Snider MD. 2003. A role for rab7 GTPase in growth factor-regulated cell nutrition and apoptosis. Mol Cell 12:796–797.
Stenmark H. 2009. Rab GTPases as coordinators of vesicle traffic. Nat Rev Mol Cell Biol 10:513–525.
Stockton RA, Schaefer E, Schwartz MA. 2004. P21-activated kinase regulates endothelial permeability through modulation of contractility. J Biol Chem 279:46621–46630.
Suetsugu S, Yamazaki D, Kurisu S, Takenawa T. 2003. Differential roles of WAVE1 and WAVE2 in dorsal and peripheral ruffle formation for fibroblast cell migration. Dev Cell 5:595–609.
Sun Y, Buki KG, Ettala O, Vaaraniemi JP, Vaananen HK. 2005. Possible role of direct Rac1-Rab7 interaction in ruffled border formation of osteoclasts. J Biol Chem 280:32356–32361.
Takaishi K, Sasaki T, Kotani H, Nishioka H, Takai Y. 1997. Regulation of cell-cell adhesion by rac and rho small G proteins in MDCK cells. J Cell Biol 139:1047–1059.
Tanida I, Ueno T, Kominami E. 2008. LC3 and Autophagy. Methods Mol Biol 445:77–88.
Wang RC, Wei Y, An Z, Zou Z, Xiao G, Bhagat G, White M, Reichelt J, Levine B. 2012. Akt-mediated regulation of autophagy and tumorigenesis through Beclin 1 phosphorylation. Science 338:956–959.
Zerial M, McBride H. 2001. Rab proteins as membrane organizers. Nat Rev Mol Cell Biol 2:107–117.

Supporting Information

Additional supporting information may be found in the online version of this article at the publisher's web-site.